JOURNAL OF MATERIALS SCIENCE 27 (1992) 5203–5208

Characteristics of mullite prepared from co-precipitated $3Al_2O_3 \cdot 2SiO_2$ powders

J. S. LEE, S. C. YU*
*Institute of Mining, Metallurgy and Materials Science, and *Department of Earth Sciences, National Cheng Kung University, Tainan, Taiwan 70101*

Diphasic gels were prepared by a precipitated process from the mixed solutions of colloidal silica and aluminium nitrate. High-purity stoichiometric mullite powders were produced by calcination of the products of these gels, with an exothermic reaction occurring at 1300 °C. The chemical and structural evolutions, as a function of thermal treatment, have been characterized by differential thermal analysis, thermogravimetric analysis, X-ray diffraction, infrared spectroscopy, and electron microscopy. The components of the co-precipitated gels react independently with increasing temperature up to the formation of mullite. The composition of mullite also varies with the temperature of thermal treatment. The calcined powders treated by ball-milling could be sintered into a high-density body, in spite of the occurrence of a small amount of glassy phase during sintering.

1. Introduction

Mullite ($3Al_2O_3 \cdot 2SiO_2$) is a characteristic constituent of traditional ceramics made from aluminosilicate and is well-known as the only stable compound in the Al_2O_3–SiO_2 system, which melts incongruently at 1828 °C [1]. According to recent studies [2, 3], mullite ceramics show little degradation in flexure strength (above 350 MPa) up to 1300 °C because of their highly covalent character. Sintered mullite is also attractive for its potential application in infrared windows [4] or low-expansion substrate manufacturing [5, 6]. However, mullite is difficult to sinter into full-density and high-purity stoichiometric bodies. To overcome these difficulties, several different processes for preparing the high-purity and active mullite powders have recently been reported [3, 7–11]. Highly pure mullite powders, however, are not yet commercially available. Even if highly pure mullite powders were available, they would be costly because of expensive raw materials and complicated preparation processes. In the present study, fine, highly purified powders were prepared by calcination of the products precipitated from a mixed aqueous solutions of aluminium nitrate and colloidal silica.

2. Experimental procedure

Colloidal silica (Ludox As-40) and aluminium nitrate were used as the precursor materials for silica and alumina, respectively. A co-precipitation process using a mixed solution of aluminium nitrate and colloidal silica was carried out at room temperature under vigorous agitation. The ammonia solution was slowly added to the mixed solution to adjust the pH of the solution to 8, so that the ratio of Al_2O_3 to SiO_2 was brought as near as possible to the ideal mullite composition value. Then the white, precipitated gels were filtered, washed, dried and calcined. Some calcined powders were ball-milled for 8 h in a nylon jar using zirconia balls and distilled water.

The surface areas of the powder were determined by the BET method (Micromeritics, Surface Area Analyser 2200) with the use of the nitrogen absorption/desorption isotherm. The crystalline phases in the calcined product were identified by X-ray diffraction (XRD), using CuK_α radiation. For the measurement of the lattice parameters of mullite, high-purity calcium fluoride powder was added to the sample as an internal standard. The reflections selected for the determination of the orthorhombic cell constants were (0 4 1), (4 0 1), (3 3 1), (4 2 1), (0 0 2) and (5 2 0). Differential thermal analysis/thermogravimetric analyses (DTA/TGA) curves of the gels were taken at a heating rate of 10 °C min^{-1} up to 1350 °C using a Rigaku TAS 100 unit. Infrared spectra of mullite were recorded from 1600–400 cm^{-1} using a Hitachi 270–30 IR spectrophotometer. The infrared samples were prepared using the KBr pellet method. The microstructures of the sintered bodies were examined using SEM techniques (Jeol JSM-35CF) after the samples had been polished, thermally etched (at 1600 °C for 40 min) and chemically etched. TEM specimens were prepared in either a thin foil or a powder form and examined at an acceleration voltage of 175 kV with a Hitachi 700H transmission electron microscope. Chemical analyses were performed on polished sections with a wavelength dispersive spectrometer (WDS). Weight percentages were calculated from the net intensities with a program correcting for the influence of atomic number, absorption, and the degree of fluorescence (ZAF-process). Green densities were computed from the weights and dimensions of the pellets. Bulk densities of the sintered pellets were measured using Archimedes' method.

0022–2461

3. Results and discussion

3.1. TGA/DTA

Thermogravimetric analysis (TGA) of gel powders exhibits a two-step weight loss as shown in Fig. 1. The first step may be assigned to the loss of absorbed water [12]. The second step in weight loss is due to decomposition of pseudoboehmite and nitrate (NH_4NO_3) [12, 13]. The total weight loss in the gel amounts to 46 wt %. There is little further weight change beyond 500 °C. The DTA heating curve obtained for the co-precipitated gel of the stoichiometric composition is shown in Fig. 2. The gels exhibit a broad endotherm around 120 °C due to the loss of water and two exothermic peaks at about 280 and at 1300 °C. The first exotherm around 280 °C is attributed to the decomposition of nitrate [13]. To characterize the origin of the second exotherm, X-ray powder diffraction patterns taken near 1300 °C are shown in Fig. 3. The XRD pattern obtained at 1200 °C is a mixture of spinel-type phases and amorphous SiO_2. On the other hand, the XRD pattern at 1300 °C shows that mullite is the predominant phase. Therefore, the XRD data indicate that the second exotherm is due to the formation of mullite. A 980 °C exotherm was reported [11] to be associated with single-phase xerogels. However, no trace of the 980 °C exotherm was found in the present study. Instead, a very broad exotherm appears from about 450 °C to above 1200 °C. It is therefore suggested that our co-precipitated gels are diphasic gels and two discrete phases, alumina and silica, are reacting independently at various temperatures up to the formation of the mullite phase.

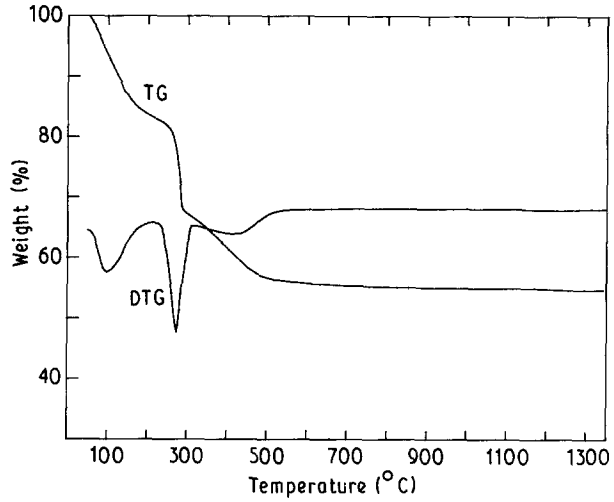

Figure 1 TG and DTG curves of the co-precipitated $3Al_2O_3 \cdot SiO_2$ gel.

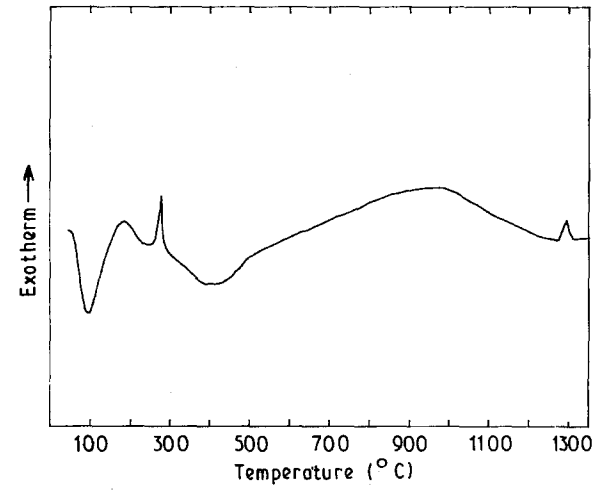

Figure 2 DTA curve of the co-precipitated $3Al_2O_3 \cdot 2SiO_2$ gel.

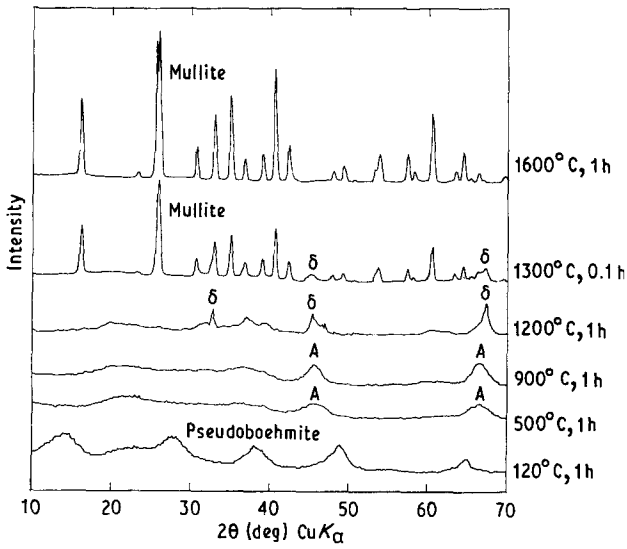

Figure 3 XRD patterns of the co-precipitated gels calcined at various temperatures. A, γ-Al_2O_3 or η-Al_2O_3; δ, δ-Al_2O_3.

3.2. XRD

To understand the sequence of phase development in the co-precipitated gels, a series of XRD patterns of the gels calcined at different temperatures was taken, as shown in Fig. 3. The XRD pattern of the gels heated at 120 °C shows the presence of pseudoboehmite and amorphous SiO_2 as two discrete phases. After 1 h at 500 °C, the XRD pattern shows that pseudoboehmite was transformed into a low-temperature form of Al_2O_3 with a cubic spinel structure, along with an amorphous band around 22° 2θ (CuK_α). At 1200 °C, δ-Al_2O_3 phase was observed in which a minor amount of θ-Al_2O_3 phase was also probably included (θ phase was observed by TEM analysis). Although both δ-Al_2O_3 and θ-Al_2O_3 transform into α-Al_2O_3 at 1150 °C [14], only mullite phase with minor amounts of δ-Al_2O_3 and/or traces of θ-Al_2O_3 were observed in the co-precipitated gel at 1300 °C. A similar phenomenon had been observed by Yoldas [15] in his studies on the Al_2O_3–SiO_2 binary system, and had been interpreted as the result of the stabilization of active alumina by silica. Only mullite peaks were detected when the present gels were heated at 1600 °C for 1 h. The phase transformation sequence for Al_2O_3 is summarized in Table I. When heated in air, pseudoboehmite first transformed into γ-Al_2O_3 below 700 °C, then into δ-Al_2O_3 around 900 °C, into θ-Al_2O_3 and α-Al_2O_3 around 1100 °C and finally into α-Al_2O_3 around 1200 °C. On the other hand, the amorphous silica gel exhibited a much simpler development history in phase change, it crystallized into cristobalite at

TABLE I Phases developed for pseudoboehmite and silica gel at different calcination temperatures

Temperature (°C)	Crystalline phases[a]	
	Pseudoboehmite	Silica gel
700	Al-spinel[b]	Amorphous
900	δ-Al_2O_3 + Al-spinel	Amorphous
1000	δ-Al_2O_3	Amorphous
1100	α-Al_2O_3 + θ-Al_2O_3	Cristobalite
1200	α-Al_2O_3	Cristobalite

[a] Identified by XRD and TEM.
[b] Al-spinel: γ-alumina or η-alumina.

TABLE II Per cent mullite at different calcination temperatures for 1 h determined by XRD analysis

Temperature (°C)	Mullite (%)
1200	trace
1250	54.8
1300	67.8
1400	82.0
1500	86.5
1600	91.5
1650	96.5
1650[a]	99.2

[a] Calcination at 1650 °C for 2 h.

about 1100 °C. The XRD results indicate that both constituents, pseudoboehmite and silica, of the present gels behave independently with temperature until the formation of mullite. Therefore, it is suggested that the co-precipitated gels are diphasic in nature.

Table II shows the amount of mullite formed at different calcination temperatures. The content was estimated based on intensities, which were, in turn, obtained by integrating the areas of the X-ray peaks. As a standard for evaluating the per cent of mullite at different calcination temperatures, part of the material was calcined at 1650 °C for 4 h to achieve a maximum conversion and growth of the mullite phase. Taking the (1 2 0)/(2 1 0) X-ray peak intensity as 100, the concentrations of mullite present in other samples were calculated as shown in Table II. This result indicates that an early stage of transformation into mullite occurred at 1250 °C and then the extent of transformation into mullite increased progressively with temperature.

Mullite formed at 1650 °C for 4 h contains 72 wt % Al_2O_3 determined by WDS analysis. The lattice parameters of this sample are $a_0 = 0.7542$ nm, $b_0 = 0.7691$ nm and $c_0 = 0.2883$ nm. Cameron [16] and Hirata *et al.* [17] reported that the value of a_0 is dependent on the alumina content of mullite. Hence, the Al_2O_3 concentration in mullite can also be estimated using the lattice parameters. Using $a_0 = 0.7542$ nm found in the present mullite sample, the Al_2O_3 content was determined to be 71.8 wt %, the result being consistent with that obtained by WDS chemical analysis; both are near the value in the ideal stoichiometric composition of mullite.

3.3. Infrared spectroscopy and TEM

Several structural changes taking place in the co-precipitated gels calcined at various temperatures were also observed by infrared spectroscopy analysis. Fig. 4 shows the infrared spectra from 4000–400 cm^{-1} before and after the major decomposition has occurred. With the gels dried at 120 °C, the principal absorption bands of pseudoboehmite are present. Also seen are absorption bands associated with amorphous SiO_2 (1100, and 470 cm^{-1}) [12, 18]. In addition, absorption bands at 3450 and 1640 cm^{-1} are prominent. The band at 3450 cm^{-1} is due to the stretching vibration of the OH radical of physically absorbed water [19]. The intensity of the 3450 cm^{-1} band

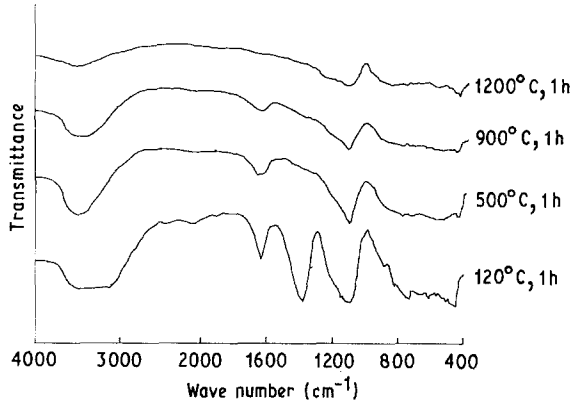

Figure 4 Infrared spectra of the co-precipitated gels of mullite composition after calcination at different temperatures.

decreased with temperature (Fig. 4), showing the removal of water on heating. On the other hand, the band at 1640 cm^{-1}, due to rotation vibration of the OH radical [19], remained unaltered in position at progressively higher temperatures, but its intensity did gradually decrease with temperature. The band at 1384 cm^{-1}, probably due to nitrate or ammonium [20], is also present as a result of the aluminium nitrate or NH_4OH solution used in the co-precipitated process. After decomposition, the infrared spectrum obtained is similar to that of the mixture of γ-Al_2O_3 and amorphous SiO_2 [17]. Okada and Otsuka [21] reported that if Al_2O_3 were substituted for SiO_2 in the amorphous solid, it would result in a shift of the Si–O vibration band from 1100 cm^{-1} towards 1000 cm^{-1}. This shift associated with the Al–Si substitution, was not detected in the infrared analysis for gels before the formation of mullite (Fig. 4). Therefore, no Al–Si spinel phase was formed in gels before the formation of mullite. Hence, the co-precipitated gels should be of a diphasic model based on Hoffman's classification [8].

Several infrared patterns of samples treated at various temperatures after mullitization are shown in Fig. 5. Cameron [16] and Okada *et al.* [22] reported the chemical composition as a function of 1130 and 1170 cm^{-1} absorbance bands. When the chemical composition of mullite is rich in Al_2O_3, the 1130 cm^{-1} peak is stronger than the 1170 cm^{-1} peak in intensity and the reverse is true as the composition approaches 60 mol% Al_2O_3. At 1250 °C, the intensity of the

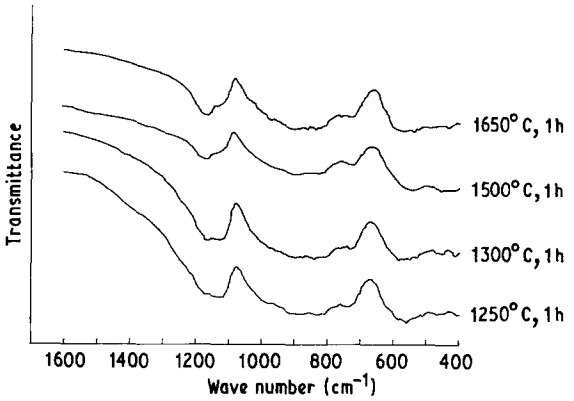

Figure 5 Infrared spectra of the co-precipitated gels of mullite composition after the formation of mullite at various temperatures.

1130 cm^{-1} band is stronger than that of the 1170 cm^{-1} band; the intensities of these two bands are almost identical at 1300 °C; when mullite is formed at higher temperatures, the intensity of the 1170 cm^{-1} band becomes stronger than that of the 1130 cm^{-1} band. This variation sequence in intensity reflects the change in chemical composition of mullite. With increasing temperature, the composition of mullite progressively approached 60 mol % Al_2O_3, the stoichiometric alumina concentration in mullite composition. Similar results were also reported elsewhere [12, 21]. Transmission electron micrographs also support this result (Fig. 6). As shown in Fig. 6, extra reflections in (k 0 l) section are diffuse and parallel to c^*. According to Cameron's study [23], the superstructure reflections in mullite are sensitive to chemical composition and vary in the length of the s vector between 60 and 66 mol % Al_2O_3. As the s vector decreases, the chemical composition approaches alumina-rich mullite. As seen in Fig. 6, it is also apparent that the chemical composition of mullite shifted towards the stoichiometric composition when mullite was formed at higher temperatures.

3.4. Calcination and sintering

The specific areas of the gels calcined at various temperatures are given in Table III. On calcination, the gels due to dehydration and thermal decomposition widen the micropores and lead to the development of a porous system in the gels [24, 25]. Hence, surface area increases with calcination temperature up to about 600 °C. With further increase in calcination temperature, particles start to undergo sintering [3] and phase transformation processes and then the surface area begins to decrease.

The sintering behaviour of the gels with and without ball-milling pretreatment is also compared in this study. The green densities of the gel powders dried at 900 °C for 1 h are 1.25 and 1.31 g cm^{-3}, respectively, for ball-milled specimens and untreated samples. The bulk densities of the bodies sintered at 1650 °C for 4 h are 3.09 and 2.59 g cm^{-3} and these densities are, respectively, 97.4 and 81.7% theoretical (3.17 g cm^{-3}). Scanning electron micrographs of these two calcined

TABLE III Surface area of gels calcined at various temperatures

Temperature (°C)	Surface area ($m^2 g^{-1}$)
120	68.2
300	188.8
600	217.4
900	109.3
1050	84.9
1200	14.9
1250	3.2

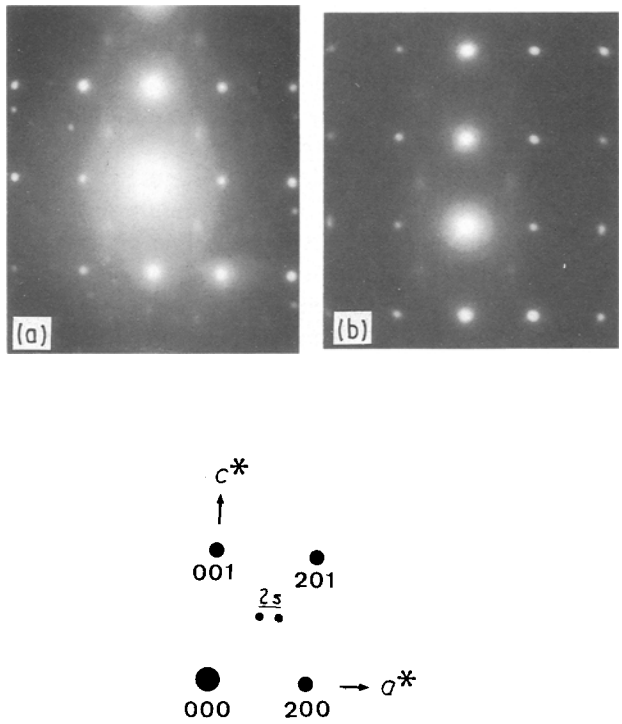

Figure 6 TEM patterns of the mullite ceramics calcined at various temperatures for 1 h: (a) 1250 °C, (b) 1500 °C, (c) index.

powders and their sintered bodies are shown in Fig. 7. Distinct agglomerations are observable in untreated calcined powders while agglomeration in ball-milled powders is almost completely absent. Untreated samples, with small pores located inside the agglomerates, shrink much faster than the non-agglomerated, ball-milling treated powders. In other words, intra-agglomerates densify more effectively than the inter-agglomerates [26]. The resultant densification of the whole body for as-calcined powders is poor; its microstructure is composed of well-densified areas separated by crack-like voids [26]. A small number of elongated grains is observed in sintered bodies for both specimens. The length of the elongated, prismatic grains is averaged to about 5 μm. The apparently unique microstructure shown in sintered bodies may be explained in terms of the small amount of liquid phase formed during sintering [13]. After a specimen was etched with 10% HF solution, a small number of cuneate-shaped scars can be observed in the sintered body (Fig. 8). This also indicates that a small amount of silica-rich glassy phase was produced in the sintered body [10]. Moreover, TEM examination also demonstrates the existence of the glassy phase (Fig. 9).

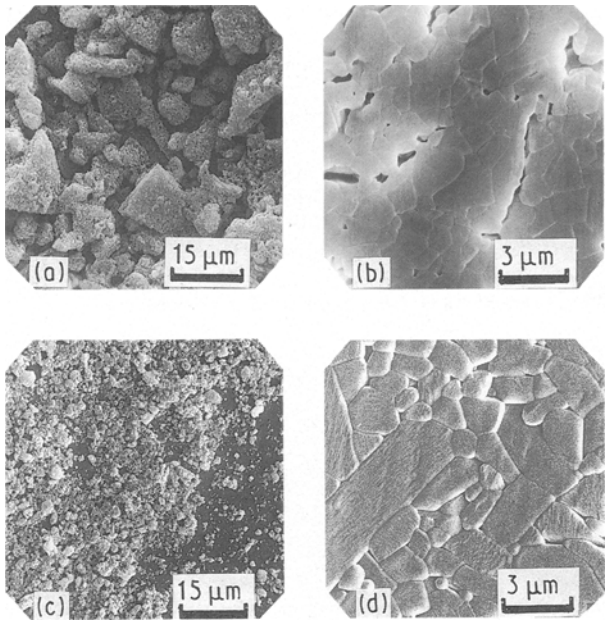

Figure 7 Scanning electron micrographs of (a, c) calcined powders (900 °C, 1 h) and (b, d) sintered bodies (1650 °C, 4 h) (right): (a, b) untreated (c, d) pretreated by ball-milling process.

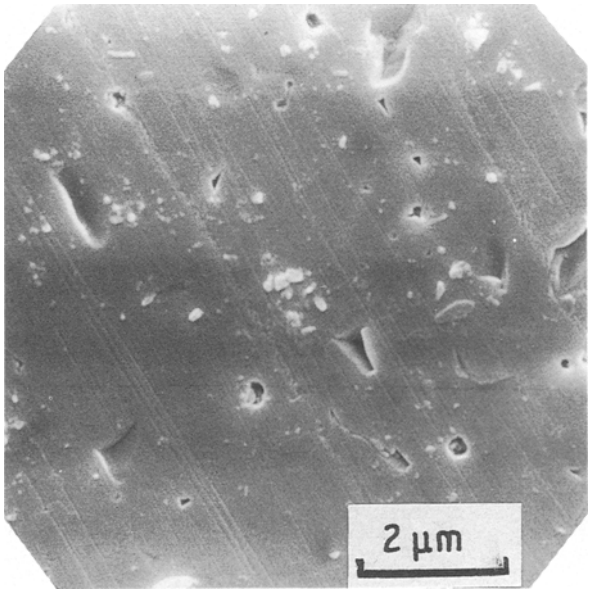

Figure 8 Scanning electron micrographs of mullite ceramics sintered at 1650 °C and chemically etched by 10% HF solution.

4. Conclusion

Mullite of stoichiometric composition has been synthesized, using a co-precipitated method, from mixed solutions of colloidal silica and aluminium nitrate. The gels are composed of pseudoboehmite and amorphous silica and are diphasic model gels in terms of Hoffman's classification, in which both constituents react independently with increasing temperature up to the formation of mullite. Initially, the mullite is alumina-rich in composition, whereas at higher temperatures, the composition gradually approaches to the stoichiometric composition of mullite ($3Al_2O_3 \cdot 2SiO_2$).

Figure 9 Transmission electron micrograph of mullite ceramics sintered at 1650 °C for 4 h showing the glassy phase in a triple junction.

The calcined powders treated by ball-milling can be sintered to a high-density body. In spite of a small amount of glassy phase occurring during sintering, it appears to be a promising high-performance ceramic.

Acknowledgement

We thank the National Science Council of Taiwan for financial assistance through grant NSC80-0416-E006-01.

References

1. A. AKSAY and J. A. PASK, *J. Am. Ceram. Soc.* **58** (1975) 507.
2. S. KANZAKI, T. KUMAZAWA, J. ASAUMI, O. ABE and H. TABATA, *Yogyo Kyokai Shi* **93** (1985) 407.
3. M. G. M. U. ISMAIL, Z. NAKAI, K. MINEGISHI and S. SOMIYA, *Int. J. High Tech. Ceram.* **2** (1986) 123.
4. S. PROCHAZKA and F. J. KLUG, *J. Am. Ceram. Soc:* **66** (1983) 874.
5. A. H. KUMAR and J. B. NIKLEWSKI, *Amer. Ceram. Soc. Bull.* **58** (1979) 1179.
6. S. KANZAKI, T. KURIHARA, S. IWAI, M. OHASHI and H. TABATA, *Yogyo Kyokai Shi* **95** (1987) 1213.
7. B. B. GHATE, D. P. H. HASSELMAN and R. H. SPRIGGS, *Amer. Ceram. Soc. Bull.* **52** (1973) 670.
8. D. W. HOFFMAN, R. ROY and S. KOMARNENI, *J. Amer. Ceram. Soc.* **67** (1984) 468.
9. T. KUMAZAWA, S. KANZAKI, J. ASAUMI, O ABE and H. TABATA, *Yogyo Kyokai Shi* **94** (1986) 485.
10. K. HAMANO, T. SATO and Z. NAKAGAWA, *ibid.* **94** (1986) 818.
11. J. A. PASK, X. W. ZHANG and A. P. THOMAS, *J. Amer. Ceram. Soc.* **70** (1987) 704.

12. M. J. HYATT and N. P. BANSAL, *J. Mater. Sci.* **25** (1990) 2815.
13. Y. KUBOTA and H. TAKAGI, *Br. Ceram. Proc.* **37** (1986) 179.
14. K. WEFERS and G. M. BELL, "Oxides and Hydroxides of Aluminum" (Technical Paper 19, ALCOA Laboratories, Pittsburgh, PA, 1972).
15. B. E. YOLDAS, *Amer. Ceram. Soc. Bull.* **59** (1980) 479.
16. W. E. CAMERON, *ibid.* **56** (1977) 1003.
17. Y. HIRATA, H. MINAMIZONO and K. SHIMADA, *Yogyo Kyokai Shi* **93** (1985) 36.
18. J. M. HUNT, M. P. WISHERD and L. C. BONHAM, *Anal. Chem.* **22** (1950) 1478.
19. H. L. HAIR, *J. Non-Cryst. Solids* **19** (1984) 299.
20. J. A. GADSDEN, "Infrared Spectra of Minerals and Related Inorganic Compounds" (Butterworths, London, 1975) pp. 24, 25, 36.
21. K. OKADA and N. OTSUKA, *J. Amer. Ceram. Soc.* **69** (1986) 652.
22. K. OKADA, Y. HOSHI and N. OTSUKA, *J. Mater. Sci. Lett.* **5** (1986) 1315.
23. W. E. CAMERON, *Amer. Mineral.* **62** (1977) 747.
24. A. L. SMITH, "Particle Growth in Suspensions" (Academic Press, London, New York, 1973) p. 38.
25. M. ASTIER and K. S. W. SING, *J. Chem. Tech. Biotechnol.* **30** (1980) 691.
26. K. HABERKO, *Ceramurgia Int.* **5** (1979) 148.

Received 3 June
and accepted 22 October 1991